

## **A Model for Predicting Coolant Activity Behaviour for Fuel-Failure Monitoring Analysis**

B.J. Lewis, J. Higgs, A. El-Jaby and W.T. Thompson  
*Department of Chemistry and Chemical Engineering, Royal Military College of Canada,  
Kingston, Ontario K7K 7B4*

F.C. Iglesias, J. Armstrong, R. Stone and R. Oduntan  
*Bruce Power, 700 University Avenue, Toronto, Ontario M5G 1X6*

### **ABSTRACT**

A mathematical treatment has been developed to predict the release of volatile fission products from operating defected nuclear fuel elements. Diffusion theory is used to account for fission-product migration in the fuel matrix and a source release into the fuel-to-clad gap. Precursor diffusion is also considered for the isotopes of I-132 and Xe-135, which have relatively long-lived precursors. The transport and release of fission products from the gap is treated as a first-order rate process as characterized by a gap escape-rate coefficient. The fission product activity in the gap and coolant follows from a mass balance considering losses due to radioactive decay, neutron transmutation and coolant purification. The activity in both the fuel-to-clad gap and coolant as a function of time can therefore be predicted during all reactor operations including reactor shutdown, startup and bundle-shifting maneuvers.

The model has been implemented as the STAR (Steady state and Transient Activity Release) code for use on personal computers with a finite-element solution of the mass transport equations using FEMLAB. The model parameters are derived from in-reactor experiments conducted with defected fuel elements containing natural and artificial failures at the Chalk River Laboratories. The STAR code has also been successfully validated against an analytical solution and benchmarked against several defect occurrences in the Bruce Nuclear Generating Station.

### **1. INTRODUCTION**

With the occurrence of defected fuel, coolant can enter into the fuel-to-sheath gap and fission products (i.e., notably the volatile species of noble gas and iodine) will be released into the primary coolant.<sup>1-5</sup> With the entry of high-pressure coolant through the defect, the fuel may be oxidized that can potentially enhance the fission product release.<sup>6,7</sup> Iodine release can also occur on reactor shutdown when the temperature in the fuel-to-sheath gap drops below the saturation temperature, permitting liquid water to dissolve the soluble iodine species in the gap resulting in an “iodine-spiking” phenomenon.<sup>8-11</sup> Iodine-rich water remaining in the gap on the subsequent startup can also be released as the size of the gap is reduced with fuel expansion.<sup>12</sup>

Defected fuel elements can release fission products and fuel debris into the primary heat transport system (PHTS),<sup>13</sup> which will increase the circuit contamination and radiation exposure during maintenance. Operation in a defected condition can cause a reduced heat transfer in the fuel-to-sheath gap as well as oxidation of the fuel, which may degrade the thermal performance of the element. In particular, fuel oxidation can result in a decrease in the thermal conductivity of the fuel and a reduced melting temperature for the hyperstoichiometric uranium.<sup>14-17</sup> It is therefore desirable to discharge defected fuel bundles as soon as possible. Hence, a better understanding of

defected fuel behaviour is required in order to develop an improved methodology for fuel-failure monitoring and coolant-activity prediction.

## 2. MODEL DEVELOPMENT

A fission product diffusion model coupled with a mass balance in the gap and coolant can be used to predict the coolant activity behaviour for both steady-state and transient reactor operation. The model can be developed for variable reactor power and coolant purification histories. In this way, the model can be matched to coolant activity trends and then used in a prognostic manner to predict the coolant activity behaviour as a function of reactor power and the coolant purification history. This tool could therefore be useful to estimate if an  $^{131}\text{I}$  action limit would be approached, which is particularly relevant since the action limit has been significantly reduced over the past number of years.

The radial diffusion equation for the concentration distribution  $C(r,t)$  at time  $t$ , based on a ‘‘Booth diffusion’’ model for an idealized fuel grain sphere of radius  $a$ , can be written as:<sup>18</sup>

$$\frac{\partial C(r,t)}{\partial t} = \frac{D(t)}{r^2} \frac{\partial}{\partial r} \left( r^2 \frac{\partial C(r,t)}{\partial r} \right) - \lambda C(r,t) + \frac{F_f(t)y}{V} \quad (1)$$

where  $\lambda$  is the radioactive decay constant ( $\text{s}^{-1}$ ),  $D$  is the diffusion coefficient for a given fission product species in the fuel matrix ( $\text{m}^2 \text{s}^{-1}$ ),  $F_f$  is the fission rate in the fuel (fission  $\text{s}^{-1}$ ),  $y$  is the cumulative fission yield (atom fission $^{-1}$ ) and  $V$  is the fuel volume for the defected element. Defining the dimensionless variable,  $\eta = r/a$ , and multiplying through by  $V$ , Eq. (1) becomes:

$$\frac{\partial u(\eta,t)}{\partial t} = \frac{D'(t)}{\eta^2} \frac{\partial}{\partial \eta} \left( \eta^2 \frac{\partial u(\eta,t)}{\partial \eta} \right) - \lambda u(\eta,t) + F_f(t)y \quad (2)$$

where  $u = CV$  and  $D' = D/a^2$ . The initial and boundary conditions are given as:

$$u(\eta,0) = 0, \quad 0 < \eta < 1, \quad t = 0 \quad (3a)$$

$$\frac{\partial u}{\partial \eta} = 0, \quad \eta = 0, \quad t > 0 \quad (3b)$$

$$u(1,t) = 0, \quad \eta = 1, \quad t > 0 \quad (3c)$$

The diffusional release to-birth rate ratio for the defected element is:

$$\left( \frac{R}{B} \right)_{dif} = \frac{4\pi a^2}{F_f y (4\pi a^3 / 3)} \left( -D \frac{\partial CV}{\partial r} \Big|_{r=a} \right) = - \frac{3D'}{F_f y} \frac{\partial u}{\partial \eta} \Big|_{\eta=1} \quad (4)$$

Equivalently, the release rate  $R_{dif}$  (atom  $\text{s}^{-1}$ ) from the defected fuel element is:

$$R_{dif} = -3D' \frac{\partial u}{\partial \eta} \Big|_{\eta=1} \quad (5)$$

Thus, the time-dependent diffusion equation in Eq. (2) can be solved by numerical methods subject to the conditions in Eqs. (3a) to (3c). The derivative of this solution (at  $\eta = 1$ ) is

subsequently used in Eq. (5). Equation (5) is the source release rate from the fuel matrix into the fuel-to-clad gap for the defected element and can be used in the mass balance for the gap:

$$\frac{dN_g(t)}{dt} = R_{dif}(t) - (\lambda + \nu(t))N_g(t) \quad (6a)$$

Here, assuming a first-order rate process for fission product release from the gap, the escape rate/leaching rate coefficient  $\nu$  ( $s^{-1}$ ) can be considered as a function of time. Also, during reactor shutdown, an enhanced leaching rate constant is used for  $\nu$  so that the model can also reproduce “iodine-spiking” phenomena. The parameter  $\nu$  can also be adjusted to reproduce convective release during other transient reactor operations. The initial condition for Eq. (6a) is:

$$N_g(t) = 0, \quad t = 0 \quad (6b)$$

The mass balance in the coolant is similarly given by:

$$\frac{dN_c(t)}{dt} = \nu(t)N_g(t) - (\lambda + \beta_p(t))N_c(t) \quad (7a)$$

with a time-dependent coolant purification rate constant  $\beta_p(t)$ . This equation is subject to the initial condition:

$$N_c(t) = 0, \quad t = 0 \quad (7b)$$

The solution of the coupled Eqs. (2), (3), (5), (6) and (7) provides a prediction of both the gap and coolant activity as a function of time for a variable fuel element linear rating/reactor power and coolant purification history. One can further follow the degradation of a fuel element with a changing value of the escape rate/leaching rate coefficient, where this parameter can be used as a tuning parameter to match the observed coolant activity data (with a knowledge of the purification flow and reactor power history).

## 2.1 Precursor Effects for I-132 and Xe-135

For isotopes that have relatively long-lived precursors, precursor effects must be considered. Thus, the model can be further generalized for the isotopes of I-132 and Xe-135 to account for precursor diffusion as well as neutron transmutation effects. The latter effect is only important for the isotope Xe-135. For parent (p)-daughter (d) diffusion, using the given variable transformation, gives:

$$\begin{aligned} \frac{\partial u_p}{\partial t} &= \frac{D'_p(t)}{\eta^2} \frac{\partial}{\partial \eta} \left( \eta^2 \frac{\partial u_p}{\partial \eta} \right) - \lambda_p u_p + F_f(t) y_p^c \\ \frac{\partial u_d}{\partial t} &= \frac{D'_d(t)}{\eta^2} \frac{\partial}{\partial \eta} \left( \eta^2 \frac{\partial u_d}{\partial \eta} \right) - (\lambda_d + \sigma_a \phi_T(t)) u_d + \lambda_p u_p + F_f(t) y_d^d \end{aligned} \quad (8)$$

where the decay of the parent isotope provides for a source of the daughter isotope. Here  $\sigma_a$  is the neutron microscopic absorption cross section for Xe-135,  $\phi_T$  is the thermal neutron flux,  $y_p^c$  is the cumulative fission yield for the parent and  $y_d^d$  the direct yield for the daughter. Both the parent and daughter are subject to the initial and boundary conditions given in Eqs. (3a) to (3c).

The diffusional source release rate into the fuel-to-sheath gap can again be evaluated from a Fick's law of diffusion:

$$R_{dif,p} = -3D'_p \left. \frac{\partial u_p}{\partial \eta} \right|_{\eta=1} \quad (9a)$$

$$R_{dif,d} = -3D'_d \left. \frac{\partial u_d}{\partial \eta} \right|_{\eta=1} \quad (9b)$$

Similarly, the coupled mass balance equations for the gap and coolant for these isotopes are given respectively by:

$$\frac{dN_{g,p}}{dt} = R_{dif,p}(t) - (\lambda_p + \nu_p(t))N_{g,p} \quad (10a)$$

$$\frac{dN_{g,d}}{dt} = R_{dif,d}(t) + \lambda_p N_{g,p} - (\lambda_d + \sigma_a \phi_T + \nu_d(t))N_{g,d} \quad (10b)$$

and

$$\frac{dN_{c,p}}{dt} = \nu_p(t)N_{g,p} - (\lambda_p + \beta_{p,p}(t))N_{c,p} \quad (11a)$$

$$\frac{dN_{c,d}}{dt} = \nu_d(t)N_{g,d} + \lambda_p N_{c,p} - (\lambda_d + \beta_{p,d}(t) + f_c \sigma_a \phi_T)N_{c,d} \quad (11b)$$

where  $f_c$  is the fraction of the PHTS mass which is in-core. The initial conditions for both the parent and daughter isotopes are again given by Eqs. (6b) and (7b).

The system of partial differential equations (PDEs) can be solved using the commercial FEMLAB software package (Version 3.1) that employs a finite-element technique.<sup>19,20</sup>

### 3. STAR CODE VALIDATION

The numerical implementation of the code can be tested against an analytical solution. The model can be further evaluated against in-reactor experiments conducted with well-characterized fuel failures in the X-2 defect loop at the Chalk River Laboratories (CRL).<sup>4</sup> This evaluation permits a good opportunity to test the model and to specifically evaluate the model parameters. Finally, the model can be validated against actual defect experience in the commercial power reactor where the number of failures, and element power rating and coolant purification histories are known.

#### 3.1. Comparison of Numerical Model Against Analytical Solutions

The numerical solution of the coupled mass transport equations can be compared to an analytical solution for the coolant activity  $A_c (= \lambda N_c)$  as derived in Ref. 21 for the long-lived isotope <sup>129</sup>I ( $\lambda = 1.40 \times 10^{-15} \text{ s}^{-1}$  and  $y = 0.00744$  atom/fission):

$$A_c(t) = \mu F_f y \left\{ \frac{1 - e^{-\phi t}}{\phi} + \left( \frac{e^{-\psi t} - e^{-\phi t}}{(\psi - \phi)} \right) \frac{3}{\psi} \left[ 1 - \sqrt{\psi} \cot \sqrt{\psi} \right] + 6\psi \sum_{n=1}^{\infty} \left( \frac{e^{-\phi t} - e^{-n^2 \pi^2 t}}{n^2 \pi^2 (n^2 \pi^2 - \psi)(n^2 \pi^2 - \phi)} \right) \right\} \quad (12)$$

where  $\mu = \lambda/D'$ ,  $\tau = D't$ ,  $\psi = v/D'$  and  $\phi = \beta_p / D'$ . This result assumes that there is no initial concentration profile in the fuel grain and no initial fission product inventory in the gap or coolant. The analytical result in Eq. (12) is also only applicable for constant coefficients of  $D'$ ,  $F_f$ ,  $v$  and  $\beta_p$ . This analysis assumes a fission rate of  $F_f = 5.96 \times 10^{14}$  fission  $s^{-1}$ , gap escape rate coefficient of  $v = 1.4 \times 10^{-6} s^{-1}$ , coolant purification rate constant of  $\beta_p = 7.05 \times 10^{-5} s^{-1}$ , empirical diffusion coefficient of  $D' = 4.57 \times 10^{-10} s^{-1}$  and PHTS mass of 244 Mg. For the analytical solution, 200 terms with STAR for the indicating a proper agreement is observed

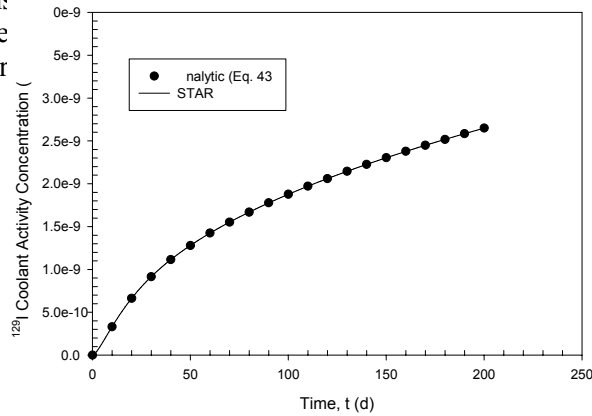


**Figure 1. Comparison of the analytic versus numerical solution for prediction of the coolant activity concentration of <sup>129</sup>I.**

### 3.2. Model Parameter Evaluation Based on X-2 Defect Experiments

An experimental program with defective CANDU-type fuel elements was carried out at the CRL.<sup>4</sup> Failed elements with various degrees of sheath damage were irradiated in separate tests in the X-2 experimental loop of the National Research Experimental (NRX) reactor. A brief summary of the fuel operating parameters for the experiments considered in the current analysis is detailed in Table 1. The experiments involved the irradiation of fuel elements that were either artificially or naturally defected. An element was artificially defected prior to irradiation with machined slits in the fuel sheathing. Other elements were characteristic of hydride failures found in power plants, which resulted from small manufacturing flaws.

**Table 1: Summary of Experiments with Single Defected Fuel Elements at CRL**

Experiment (Element)	Test (Defect) Description	Defect Size (mm <sup>2</sup> )		Linear Power (kW/m)	Burnup (MWh/kgU)		Defect Residence Time (Effective Full Power Days)	Fuel Loss (g)
		Initial	Final		Initial	Final		

<b>A. Artificially-Defected Fuel</b>								
FFO-103 (A3N)	23 through-wall slits in a helical pattern along sheath (each slit 36 mm × 0.3 mm)	272	1490 <sup>a</sup>	48	0	18	15	~65
<b>B. Naturally-Defected Fuel</b>								
FFO-102-1 (A7A)	Irradiation of elements with porosity in end caps	b	-	16	0	68	153	N/A
(A7E)		b	-	64	0	37	24	N/A
FFO-102-3 (A7A)	Reirradiation of element with incipient hydriding at low power	b	-	23	68	130	263	N/A
FFO-102-2 (A7E)	Reirradiation of element with through-wall hydriding at high power (Cracked hydride blisters at one end of element)	11	300 <sup>b</sup>	67	37	67	19	3.5
FFO-110 (A7A)	Power cycling of an element with through-wall hydriding	~0.5	-	14 to 26	130	140	281	N/A
FFO-109 (Phase 2) (A7A)		-	~0.5	22 to 38	140	155	300	<0.1

a. Slits enlarged during irradiation due to fuel expansion (defect size estimated from post-irradiation examination).

b. Primary defect size for A7A (0.4 µm) and A7E (1.4 µm).

N/A Not available (no metallography performed at this stage of irradiation).

The X-2 defect experiments, which cover various operating conditions and different types of fuel failures, can provide data for validation of the model and an estimation of the model parameters. The multi-slit element A3N in experiment FFO-103 represents a “worst-case” defect irradiated at a relatively high power of 48 kW/m where there is essentially no sheathing barrier so that fuel oxidation is maximized. Element A7A is a typical hydride failure that was previously irradiated in FFO-102-1 and FFO-102-3 and subsequently power-cycled in experiments FFO-110 and FFO-109 (Phase II) at low (14-26 kW/m) and intermediate (22-38 kW/m) linear powers. Finally, element A7E, which was irradiated in experiment FFO-102-1 and then re-irradiated at a very high linear power of ~67 kW/m in FFO-102-2 (which is beyond normal commercial operating conditions), represents a severe hydride failure. Thus, these experiments cover a very broad range of operating powers and states of element deterioration.

The input conditions for the model were based on operational data.<sup>20,22-25</sup> The fission yields and decay constant were taken from Ref. 3. For Xe-135, a neutron absorption rate of  $\sigma_a \phi_T = 7.862 \times 10^{-5} (P/51) \text{ s}^{-1}$  was derived from a Wescott analysis of the X-2 loop experiments (i.e., as normalized to a linear power of  $P = 51 \text{ kW/m}$ ).

The gap escape-rate coefficients were taken from a previous steady-state analysis of the X-2 experiments in Ref. 3 (see Table 2). However, these coefficients were increased by a factor of ~100 with reactor startup to account for enhanced (convective) release as the fuel-to-clad gap is reduced with fuel-pellet expansion. For the multi-slit element, A3N, this effect was ignored since the gap inventory is expected to be much less due to the presence of many defects. On reactor shutdown, in order to model the “iodine-spiking” phenomena, an enhanced gap escape-rate coefficient of  $2 \times 10^{-5} \text{ s}^{-1}$  was used as suggested in Ref. 8. This leaching rate coefficient accounted for enhanced ionic diffusion/natural convective transport with the presence of liquid water in the gap. However, no release of noble gases is assumed to occur in the vertical elements with the presence of liquid water in the gap. In accordance with the observations in Ref. 26, Te-132 is only assumed to be washed out of the gap on reactor shutdown.

The empirical diffusion coefficients were fit to the coolant activity concentration data for the various experiments. This parameter accounts for the effect of intergranular (solid-state) diffusion, intra and inter-granular bubble coalescence, grain-boundary interlinkage and grain-boundary sweeping. The fitted results are slightly different from that obtained in the previous steady-state analysis of Ref. 3 since the latter analysis only pertains to a small sampling period whereas the current analysis requires an average value over the whole irradiation period since the diffusion coefficient changes with increased fuel oxidation effects. Thus,  $D'$  (in  $\text{s}^{-1}$ ) was derived from a previous correlation as a function of the linear fuel element power  $P$  (in kW/m) based on sweep gas experiments with unoxidized fuel;<sup>27</sup> however, this relation is multiplied by a simple enhancement factor ( $\xi_{X-2} \cdot \xi_{tr}$ ) to account for fuel oxidation effects:

$$D'(P) = (\xi_{X-2} \cdot \xi_{tr}) \exp\{a_0 + a_1 P + a_2 P^2\} \quad (13)$$

where  $a_0 = -30.856311$ ,  $a_1 = -0.039332$  and  $a_2 = 2.056960 \times 10^{-3}$ . Here  $\xi_{X-2}$  is a correction factor used to match the steady-state value for oxidized fuel and  $\xi_{tr}$  is a tuning factor employed for the current transient analysis to reproduce an average value for the complete irradiation period (see Table 2 and Figure 2(a)). The same diffusion coefficient is used for all species (i.e., tellurium, iodine and noble gas species). The effect of fuel cracking on reactor shutdown/startup, however, has not been modelled in the current simulations since this effect is expected to be of less importance.<sup>12,28</sup>

A comparison of the predicted and measured trends for the coolant activity concentration for the various experiments for several selected isotopes of iodine and noble gas is shown in Figure 3 to Figure 6. There is generally a good agreement between the model results and experimental data for all isotopes. As demonstrated in Figure 3 to Figure 6, precursor effects must be considered for the coolant activity concentration prediction of I-132 and Xe-135.

**Table 2: Evaluation of Model Parameters**

Experiment	O/U Ratio	Linear Power <sup>a</sup> (kW/m)	Model Parameter									
			Empirical Diffusion Coefficient, $D'$ (s <sup>-1</sup> )					Escape-Rate Coefficient, $\nu$ (s <sup>-1</sup> )				
			Steady-State		Current <sup>b</sup>	$\xi_{X-2}$	$\xi_{I-132}$	Steady-State		Current		
			I	NG				I	NG	I	NG	
FFO-103	2.28	51.0	$5.01 \times 10^{-9}$	$2.14 \times 10^{-9}$	$3.01 \times 10^{-8}$	4450.6	6.0	$1.8 \times 10^{-4}$	$2.3 \times 10^{-4}$	$1.8 \times 10^{-4}$	$2.3 \times 10^{-4}$	
FFO-110	-	26.0	$6.55 \times 10^{-12}$	$6.38 \times 10^{-12}$	$6.55 \times 10^{-12}$	114.01	1.0	-	-	$6.8 \times 10^{-8}$	$9.3 \times 10^{-7}$	
FFO-109-2	-	33.0	$6.86 \times 10^{-11}$	$5.00 \times 10^{-11}$	$1.10 \times 10^{-10}$	673.20	1.6	$6.8 \times 10^{-8}$	$4.9 \times 10^{-5}$	$6.8 \times 10^{-8}$	$4.9 \times 10^{-5}$	
FFO-102-2 <sup>c</sup>	~2.14	66.6	$4.46 \times 10^{-10}$	$2.56 \times 10^{-9}$	$3.80 \times 10^{-9}$	143.11	1.0	$2.5 \times 10^{-6}$	$8.4 \times 10^{-6}$	$2.5 \times 10^{-6}$	$8.4 \times 10^{-6}$	

(a) Linear power at which steady-state diffusion coefficient was measured or maximum linear power; (b) Evaluated with Eq. (13); (c) As detailed in Ref. 20, the escape rate coefficients were reduced by a factor of 3 (iodine) and increased by a factor of 1.5 (noble gas) during part of the irradiation history from the steady-state values proposed in Ref. 3.

As shown in Table 2 and Figure 2(a), the fitted diffusion coefficient for FFO-103 is specifically enhanced with a higher oxygen-to-uranium (O/U) ratio. A comparison of the (steady-state) empirical diffusion coefficients in Ref. 3 with the current fitted values for the X-2 analysis is also shown in Figure 2(b) and listed in Table 2. The empirical diffusion coefficient for experiment FFO-109-2 is in fact “representative” of that for typical commercial power reactor experience where:

$$D'(P) = 4.28 \times 10^{-11} \exp\{-0.03933 \cdot P + 0.00205696 \cdot P^2\} \quad (14)$$

The range of the empirical diffusion coefficients seen in Figure 2(a) is consistent with that seen for intact versus defected fuel rods in German Pressurized Water Reactors (PWR) and Boiling Water Reactors (BWR).<sup>29</sup>

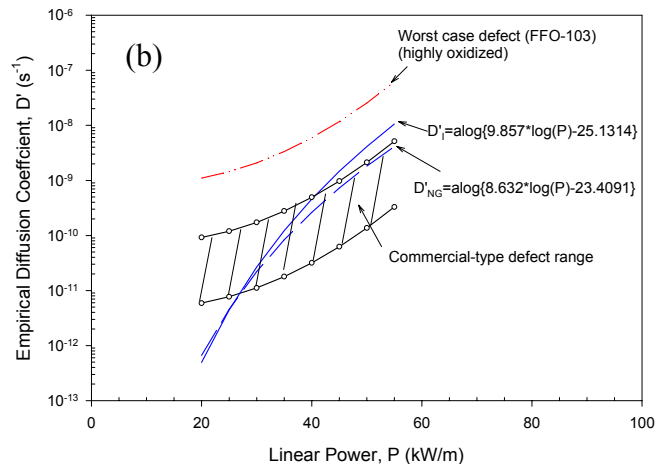
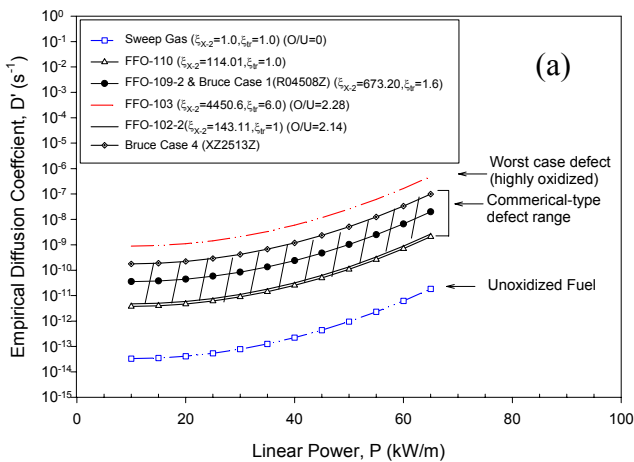


**Figure 2. Empirical diffusion coefficients as a function of the fuel element linear power for: (a) unoxidized and oxidized fuel in the current analysis; (b) comparison between the previous steady-state analysis and current work.**

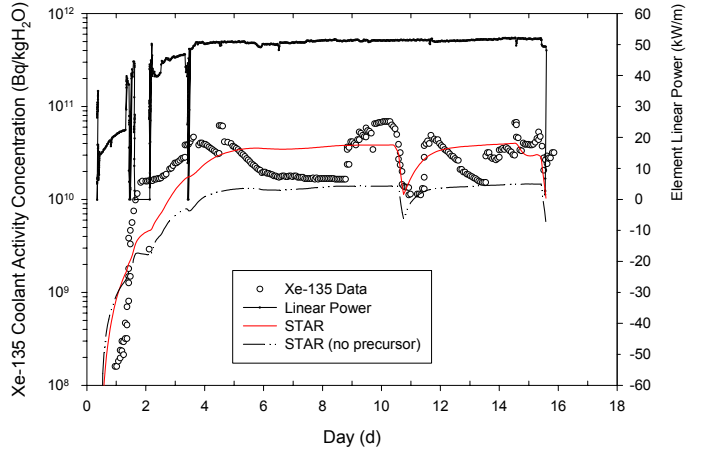
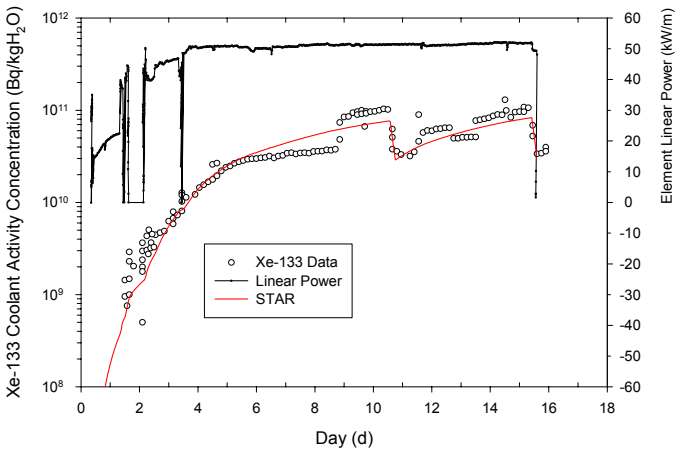
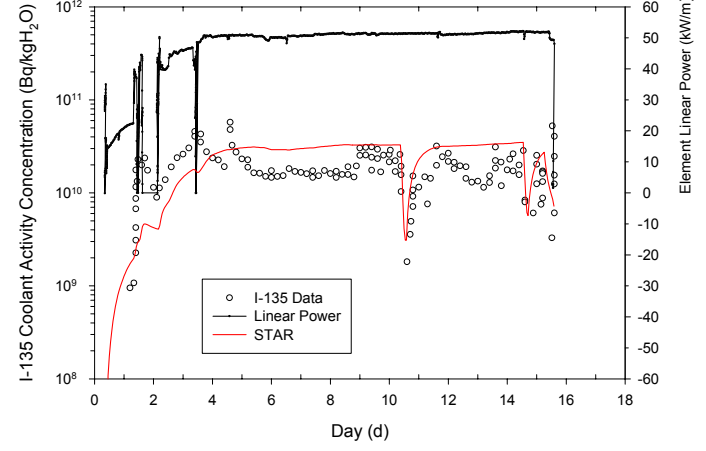
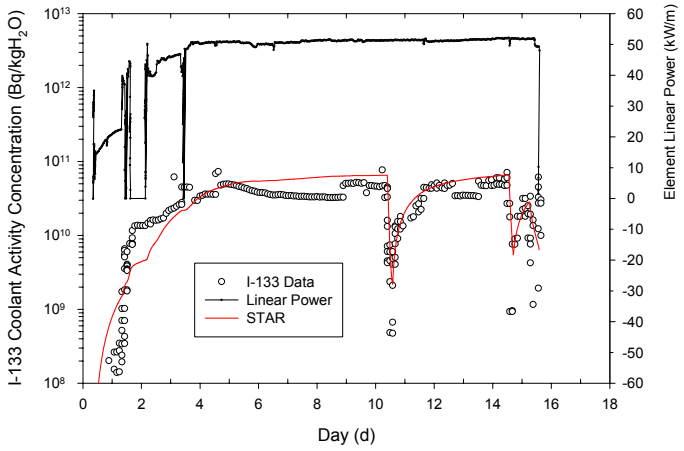
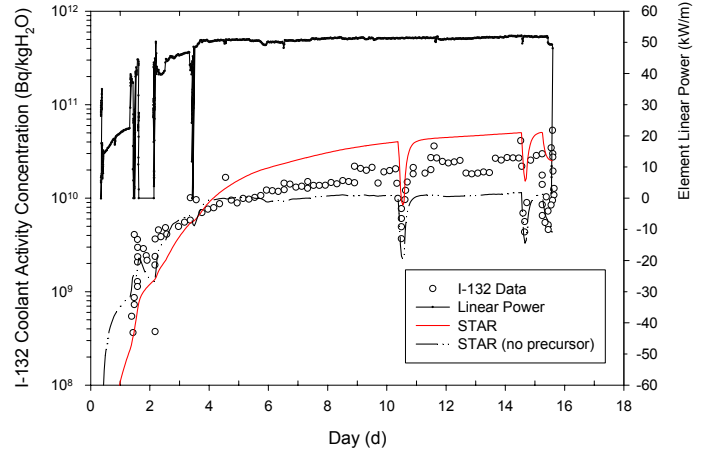
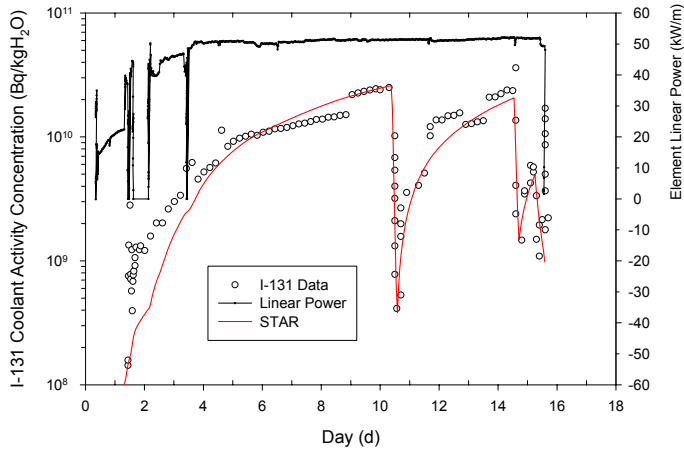


**Figure 3. Comparison between the measured and predicted coolant activity concentration history for iodine and noble gas species for experiment FFO-103.**

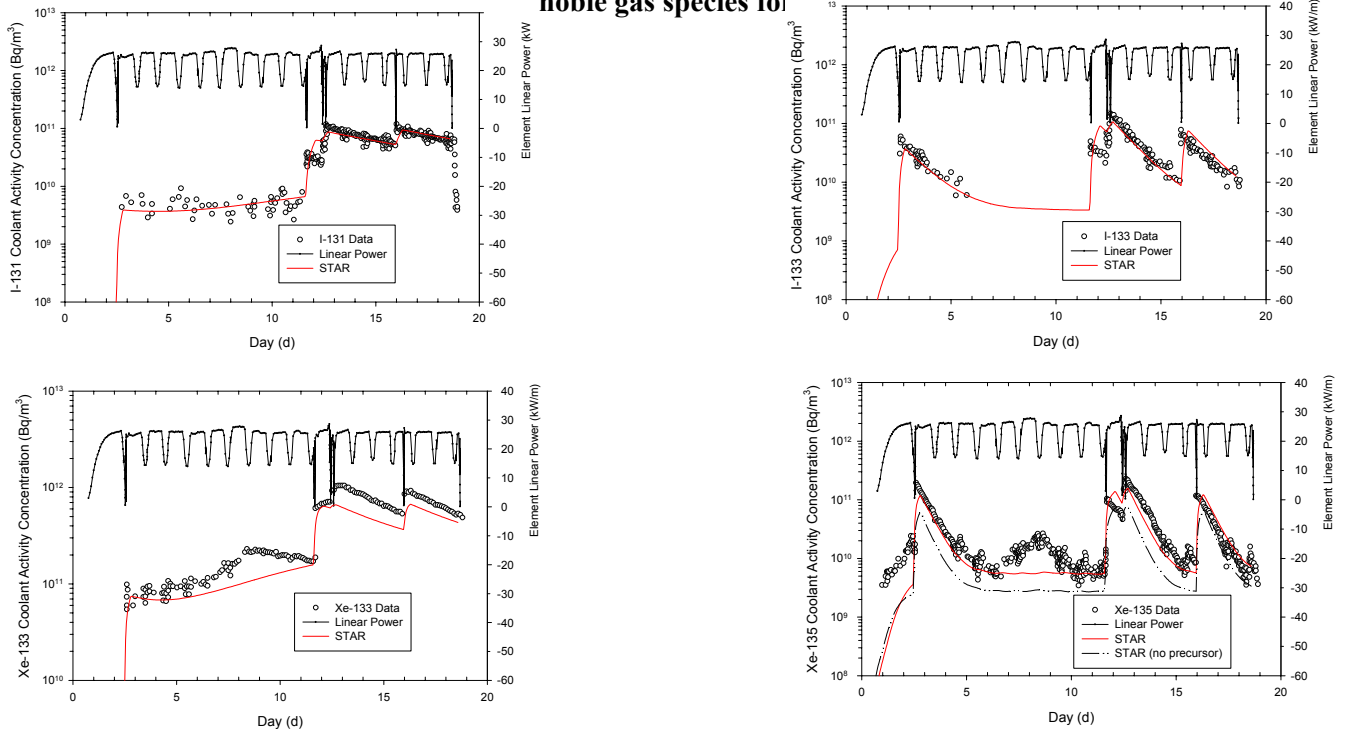


**Figure 4. Comparison between the measured and predicted coolant activity concentration history for iodine and noble gas species for experiment FFO-110.**

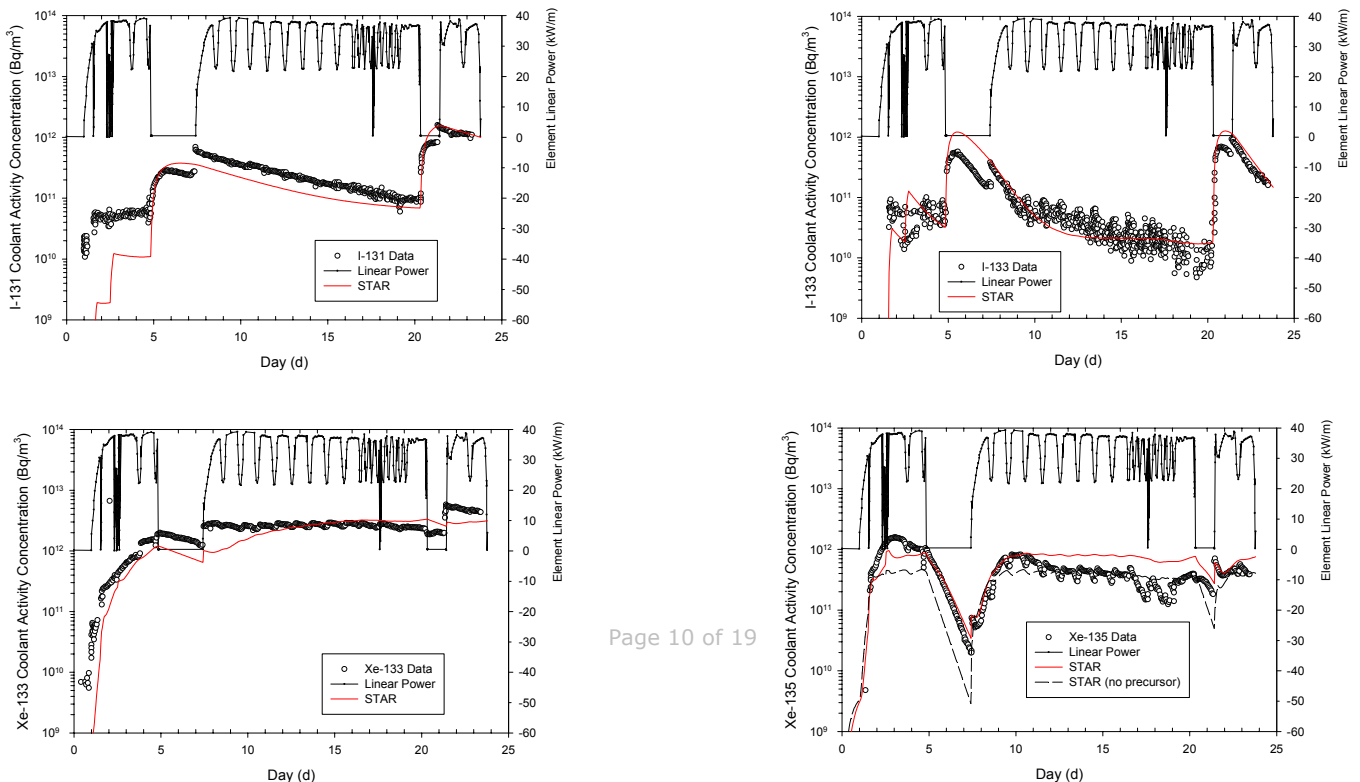


**Figure 5. Comparison between the measured and predicted coolant activity concentration history for iodine and noble gas species for experiment FFO-109-2.**

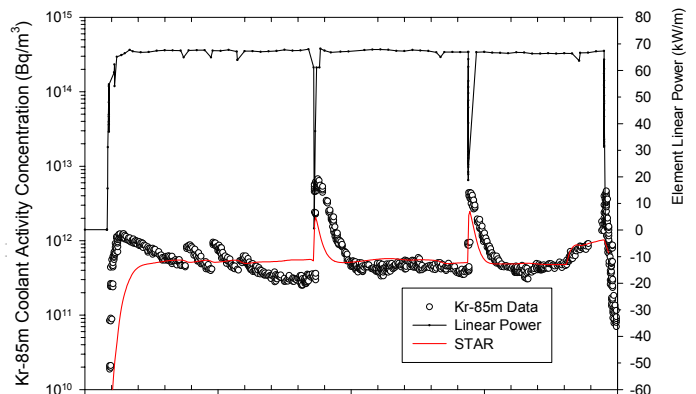
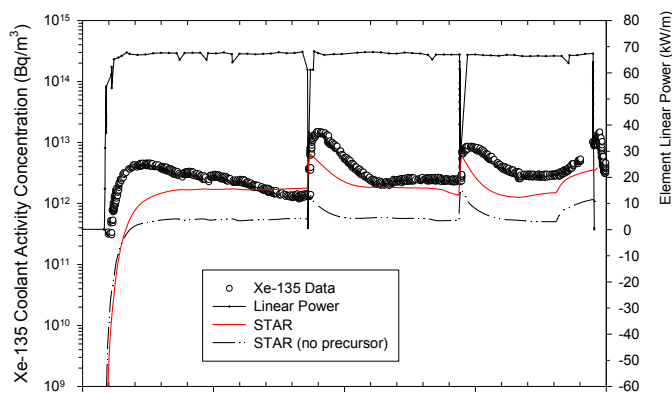
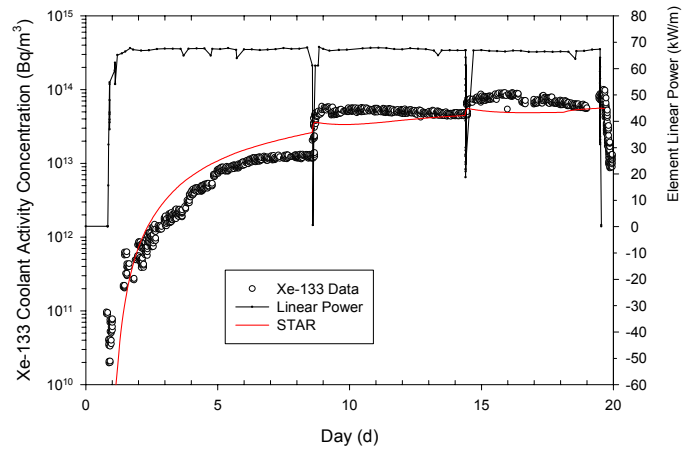
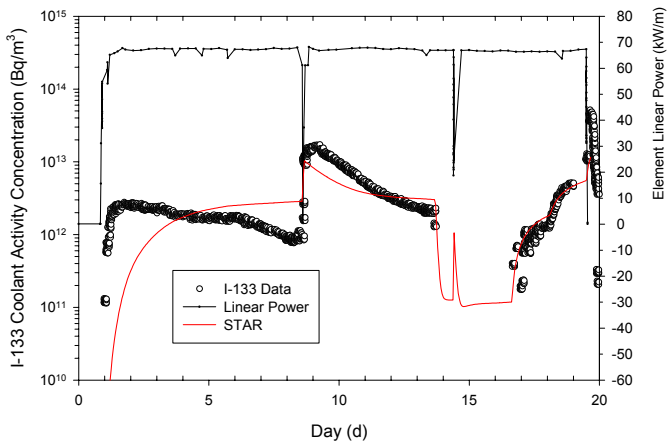
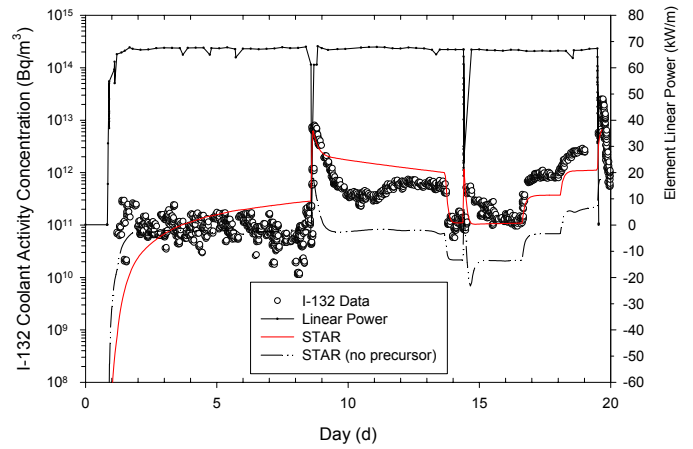
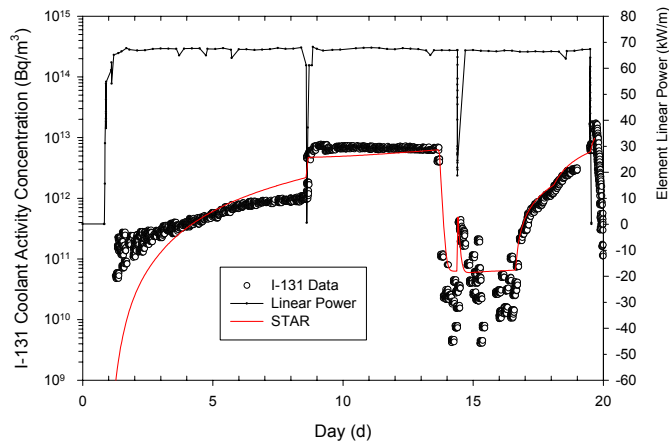


**Figure 6. Comparison between the measured and predicted coolant activity concentration history for iodine and noble gas species for experiment FFO-102-2.**

### 3.3 Commercial Reactor Application

Representative fitting parameters for the fission-product release model have been evaluated by benchmarking the model against coolant activity data derived from well-characterized failures in the X-2 defect program (Section 3.2). The model can now be applied for coolant activity analysis in the commercial Bruce reactor for several defected fuel cases.

A systematic assessment of the PHTS radionuclide activity in Bruce B units was carried out in Ref. 30. Two representative cases were selected from this survey for analysis with STAR. These two specific cases were chosen since a single failure was known to be present in the core at the given time. The irradiation histories of the defect elements, as well as the purification operations, were determined from the historical data. The defected element linear powers were calculated from bundle power histories obtained with SORO. Radionuclide activities of I-131 and Xe-133 were monitored in the commercial reactor. These activities were assessed with grab sample monitoring from the Chemistry Environmental Management (CEM) Database and with on-line gaseous fission product (GFP) monitoring from the Plant Information (PI) Database. Only activity levels greater than a preset threshold limit of 1 Ci were stored in the PI database whereas lower activities were available in the CEM database. Finally, the Fuels Inspection Database (FID) provided a documentation of the post-irradiation examination for these elements to enable a characterization of the defect sizes. These two cases as detailed in Table 3 can therefore be used to benchmark the STAR code for commercial operation with defected fuel.

**Table 3: Details of Selected Cases of Commercial Defect Experience as used for STAR Validation**

Survey Case Number <sup>a</sup>	Failed Fuel Identification	Date (Position) <sup>b</sup>		Fuel Shift Dates (Position) <sup>b</sup>		Defect Description	
		Loading	Discharge	Shift 1	Shift 2	Primary Cause	Examination Details
1	R04508Z	20 Nov 99 (Unit 5-M03/01)	8 May 00 (M03/13)	13 Mar 00 (M03/05)	7 May 00 (M03/13)	Incomplete weld	Broken hydride blister (5 mm diameter). Only defect on element.
4	XZ2513Z	18 Jan 03 (Unit 6-U06/04)	17 Jun 03 (U06/12)	11 Apr 03 (U06/08)		Debris Fretting	Fully-separated upstream end cap. Small fretted hole in sheath in weld upset (0.1 mm × 0.1 mm)

a. Case number as given in Ref. 30.

b. Channel/bundle position.

The actual element linear powers and purification flows for these cases are shown in Figure 8 and Figure 7. These parameters as input into STAR are also shown along with the model input of the gap escape rate coefficients. The gap escape rate coefficients were fitted to reproduce the coolant activity concentrations (which are consistent with those values obtained for the X-2 experiments in Table 2). The empirical diffusion coefficients are also similar to those for the X-2 experiments in Figure 2(a). The analysis for the Bruce Case 1 uses Eq. (14), whereas the Bruce Case 4 employs a coefficient that is five times greater. The same diffusion coefficient was used for both iodine and noble gas. A slightly larger coefficient had to be used for element XZ2513Z (Case 4) since the defect was very large with a separated end cap leading, presumably, to greater fuel oxidation. For instance, the rare gas diffusion coefficient in hyperstoichiometric  $UO_{2+x}$  is seen to increase through the vacancy-enhanced component as the square of the stoichiometry

deviation.<sup>14</sup> However, this coefficient was still lower than that observed for the “worst case” defect in experiment FFO-103. The same diffusion coefficient as for experiment FFO-109-2 was

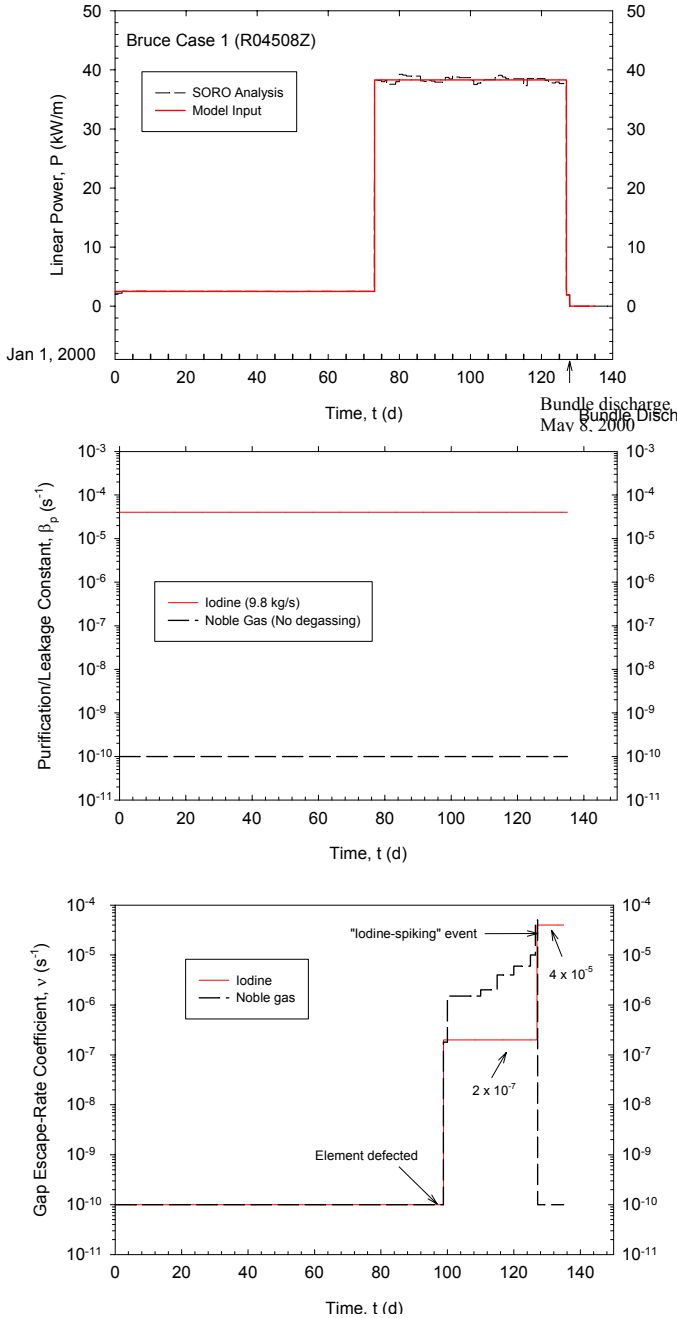


**Figure 8. Input parameters for the simulation of Bruce Case 1.**

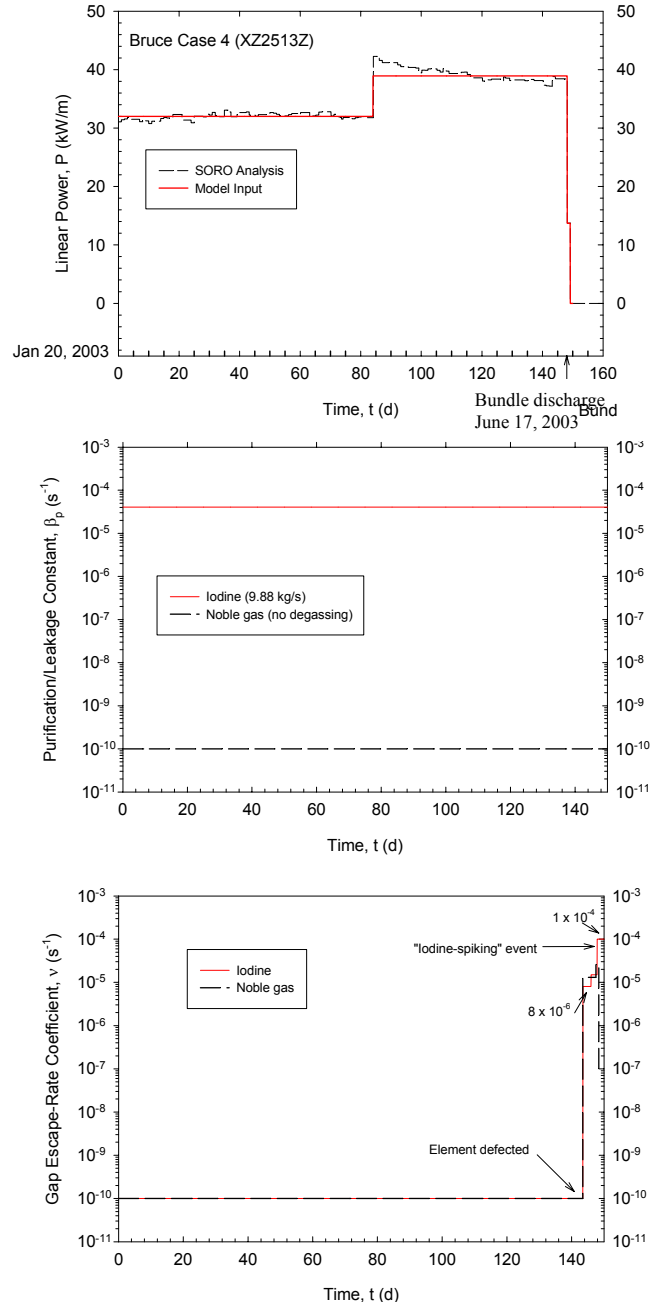


**Figure 7. Input parameters for the simulation of Bruce Case 4.**

employed for element R04508Z (Case 1) since it had a small hydride blister. Prior to failure of the elements, an unoxidized diffusion coefficient (i.e., as determined from the sweep gas experiments in Figure 2(a) with Eq. (13) for  $\xi_{X-2} = \xi_{tr} = 1$ ) was employed in the simulation.

Excellent agreement is seen in the comparison of the measured coolant activity concentrations (from GFP and CEM samples) for the monitored isotopes of I-131 and Xe-133 with the predicted quantities as shown in Figure 9 and Figure 10. The model is also able to predict “iodine-spiking” phenomenon with bundle shifting/reactor shutdown. Spiking of noble gases is further modeled

with STAR during transient operation. Interestingly, noble-gas spiking is also observed on shutdown for the commercial defects (i.e., for the horizontal orientation of the CANDU fuel channel), whereas enhanced releases for the noble gases only occurred on shutdown with the vertically-oriented elements in the X-2 defect loop (where presumably noble gases became trapped at the top of the element when liquid water filled the element).

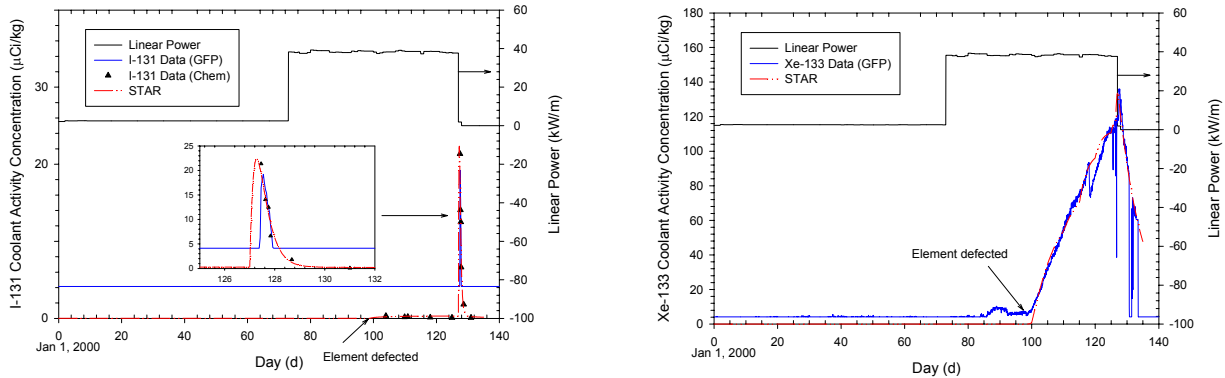


**Figure 9. Comparison between the measured and predicted coolant activity concentration history for iodine and noble gas species for Bruce Case 1.**

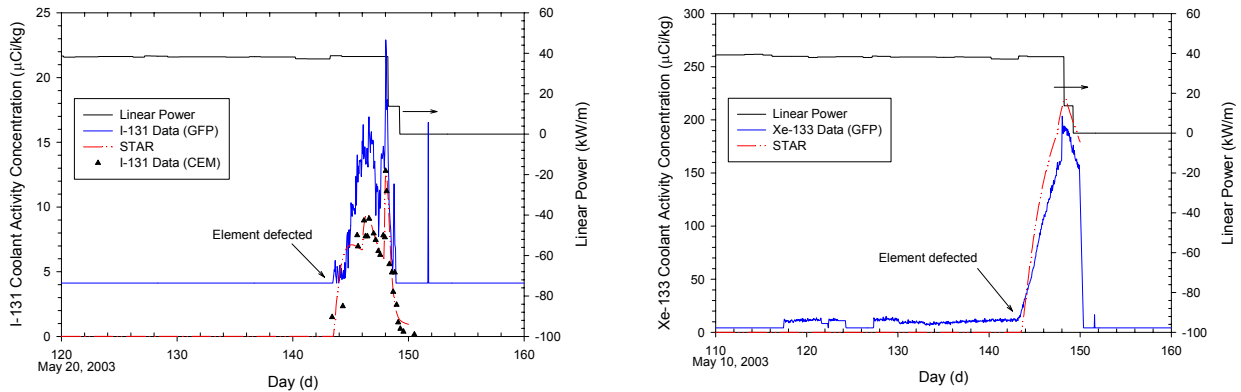


**Figure 10. Comparison between the measured and predicted coolant activity concentration history for iodine and noble gas species for Bruce Case 4.**

#### 4. CONCLUSIONS

1. A general time-dependent model entitled STAR (Steady-state and Transient Activity Release) has been developed to detail the coolant activity behaviour of the short-lived iodine and noble gas species during steady reactor operation, as well as for transient conditions of reactor shutdown, startup and bundle-shifting operations. The fission

product transport model is based on solid-state diffusion in the fuel matrix and first-order kinetics in the fuel-to-sheath gap. The effect of precursor diffusion and neutron absorption has been incorporated into the treatment. The loss of fission products by radioactive decay and coolant purification (i.e., ion exchange and degassing operations) has also been considered. This model has been solved numerically using the FEMLAB finite-element solver. The model can be used for prediction of the activity in both the fuel-to-clad gap and primary coolant for defective fuel as a function of time.

2. The code has been tested against an analytical solution of the coolant activity. The model has been benchmarked against well-characterized in-reactor experiments with defected elements conducted in the X-2 defect loop facility at the CRL. The model has been further validated against several defect occurrences in the commercial Bruce NGS (where a single failure was present). The code is successfully able to predict the iodine and noble gas inventory during steady operation as well as enhanced releases in the primary coolant that occur during reactor shutdown, startup and bundle shifting operations.

## **5. ACKNOWLEDGEMENTS**

The authors would like to acknowledge the assistance and support of the Nuclear Safety Analysis and Support Department of Bruce Power. The authors also wish to thank M.R. Floyd (CRL) for discussions on defected fuel behaviour. The authors also acknowledge the data made available under the joint Atomic Energy of Canada Limited-Ontario Hydro X-2 Defect Program.

## **REFERENCES**

1. B.J. Lewis, C.R. Phillips and M.J. Notley, "A Model for the Release of Radioactive Krypton, Xenon, and Iodine from Defective UO<sub>2</sub> Fuel Elements", Nucl. Technol. 73 (1986) 72-83.
2. B.J. Lewis, "Fundamental Aspects of Defective Nuclear Fuel Behaviour and Fission Product Release", J. Nucl. Mater. 160 (1988) 201-217.
3. B.J. Lewis, R.J. Green and C. Che, "A Prototype Expert System for the Monitoring of Defected Nuclear Fuel Elements in Canada Deuterium Uranium Reactors", Nucl. Technol., 98 (1992) 307-321.
4. B.J. Lewis, R.D. MacDonald, N.V. Ivanoff and F.C. Iglesias, "Fuel Performance and Fission Product Release Studies for Defected Fuel Elements", Nucl. Technol., 103 (1993) 220-245.
5. B.J. Lewis, "An Overview of Defective Fuel Analysis in CANDU and Light Water Reactors," 6th Int. Conf. on CANDU Fuel, ISBN 0-919784-62-3, Niagara Falls, Ontario, Vol. 1, Sept. 26-29, 1999, p. 403-427.
6. B.J. Lewis, F.C. Iglesias, D.S. Cox and E. Gheorghiu, "A Model for Fission Gas Release and Fuel Oxidation Behaviour for Defected UO<sub>2</sub> Fuel Elements", Nucl. Technol. 92 (1990) 353-362.
7. B.J. Lewis and B. Szpunar, "Modelling of Fuel Oxidation Behaviour in Operating Defective Fuel Rods," Seminar on Fission Gas Behaviour in Water Reactor Fuels, Cadarache, France, September 26-29, 2000.
8. B.J. Lewis, D.B. Duncan and C.R. Phillips, "Release of Iodine from Defective Fuel Following Reactor Shutdown", Nucl. Technol. 77 (1987) 303-312.

9. B.J. Lewis, "A Model for Calculating the I-131 Release from Defective Fuel for Steady-State and Reactor Shutdown Conditions", ISBN 0-919784-25-9, Proceedings of the Third International Conference on CANDU Fuel, Chalk River, Canada, 4-6 October 1992, p. 6-11 to 6-22.
10. B.J. Lewis, F.C. Iglesias, A.K. Postma and D.A. Steininger, "Iodine Spiking Model for Pressurized Water Reactors," J. Nucl. Mater. 244 (1997) 153-167.
11. W.N. Bishop, "Iodine Spiking," EPRI NP-4595, Electric Power Research Institute, 1986.
12. B.J. Lewis, R.D. MacDonald and H.W. Bonin, "Release of Iodine and Noble Gas Fission Products from Defected Fuel Elements during Reactor Shutdown and Startup", Nucl. Technol. 92 (1990) 315-324.
13. B.J. Lewis, "Fission Product Release from Nuclear Fuel by Recoil and Knockout", J. Nucl. Mater. 148 (1987) 28-42.
14. B.J. Lewis, B. Szpunar and F.C. Iglesias, "Fuel Oxidation and Thermal Conductivity Model for Operating Defective Fuel Rods," J. Nucl. Mater. 306 (2002) 30-43.
15. W.T. Thompson, B.J. Lewis, F. Akbari and D.M. Thompson, "Part I: Thermodynamics of Uranium Oxidation in Support of Kinetics Model For Operating Defective Fuel Elements," 8th International Conference on CANDU Fuel, Honey Harbour, Ontario, September 21-24, 2003.
16. B.J. Lewis, W.T. Thompson, F. Akbari and C. Thurgood, "Part II: Fuel Oxidation Kinetics Model For Operating Defective Fuel Elements," 8th International Conference on CANDU Fuel, Honey Harbour, Ontario, September 21-24, 2003.
17. B.J. Lewis, W.T. Thompson, F. Akbari, D.M. Thompson, C. Thurgood and J. Higgs, "Thermodynamic and Kinetic Modelling of the Fuel Oxidation Behaviour in Operating Defective Fuel," J. Nucl. Mater. 328 (2004) 180-196.
18. A.H. Booth, "A Suggested Method for Calculating the Diffusion of Radioactive Rare Gas Fission Products from  $\text{UO}_2$  Fuel Elements and a Discussion of Proposed In-Reacto Experiments That May Be Used to Test Its Validity," AECL-700, Atomic Energy of Canada Limited (1957).
19. "FEMLAB User's Guide," COMSOL AB, Burlington, MA, USA, 2004.
20. B.J. Lewis, "Steady-State and Transient Activity Release (STAR) Code for Defected Fuel, Volume 1: Theory Manual," contract report for Bruce Power, July 2005.
21. B.J. Lewis and A. Husain, "Modelling of the Activity of I-129 in the Primary Coolant of a CANDU Reactor," J. Nucl. Mater. 312 (2003) 81-96.
22. R.L. da Silva, "Irradiation of a CANDU  $\text{UO}_2$  Fuel Element with Twenty-Three Machined Slits Cut Through the Zircaloy Sheath," Atomic Energy of Canada Limited report, AECL-8260, September 1984.
23. R.L. da Silva and N. Macici, "The Irradiation Performance of a Naturally Defective CANDU  $\text{UO}_2$  Fuel Element Power Cycled Between Linear Powers of 25-14 kW/m and 38-22 kW/m in the X-2 Loop of NRX," Chalk River Nuclear Laboratories report CRNL-2674, September 1984.
24. M.R. Floyd, "Behaviour of a Zircaloy-Sheathed  $\text{UO}_2$  Fuel Element Containing an End Cap Porosity Defect Irradiated in the X-1 and X-2 Loops at an Average Linear Heat Output of 23 kW/m", Chalk River Nuclear Laboratories report CRNL-2687, July 1984.
25. B.J. Lewis, "Behaviour of a Zircaloy-Sheathed  $\text{UO}_2$  Fuel Element Containing a Porous End Plug Defect and Exhibiting Secondary Sheath Hydriding Irradiated in Pressurized Light Water at a Linear Power of 67 kW/m", Chalk River Nuclear Laboratories report CRNL-2473, May 1983.

26. R.L. Da Silva, D.R. McCracken and K.J. Monserrat, "Behaviour of Depositing Fission Products Release from Defective Fuel, in: *Advances in Ceramics*, Vol. 17, *Fission-Product Behaviour in Ceramic Oxide Fuel*, edited by I.J. Hastings, American Ceramic Society, Columbus, Ohio (1986), p. 107-120.
27. B.J. Lewis, "Visual\_DETECT: A Software Package For Fuel-Failure Monitoring For GFP/Grab Sampling Analysis," Volume 1: Theory Manual, Contract report to Bruce Power, December 2003.
28. C.E.L. Hunt and B.J. Lewis, "Transient Fission Product Release During Reactor Shutdown and Startup", *Proceedings of the 4th International Conference on CANDU Fuel*, ISBN 0-919784-52-6, Pembroke, Ontario, October 1-4, 1995, p. 4B 1-14.
29. E. Schuster et al., "Escape of Fission Products from Defective Fuel Rods of Light Water Reactors," *Nucl. Eng. and Design* 64 (1981) 81.
30. R. Oduntan, "Fission Products Behaviour in the PHTS Following Fuel Failure Occurrence," Bruce Power report NK29-REP-37000 P NSAS, March 2005 (draft).